



Dual-target platinum(IV) complexes exhibit antiproliferative activity through DNA damage and induce ER-stress-mediated apoptosis in A549 cells

Meng Wang^{a,1}, Zhikun Liu^{c,1}, Xiaochao Huang^{a,d,*}, Yuanhang Chen^a, Yanming Wang^a, Jing Kong^a, Yong Yang^a, Chunhao Yu^a, Jin Li^a, Xu Wang^{b,d,*}, Hengshan Wang^{d,*}

^a Jiangsu Key Laboratory of Regional Resource Exploitation and Medicinal Research, and National & Local Joint Engineering Research Center for Mineral Salt Deep Utilization, Huaiyin Institute of Technology, Huaian 223003, China

^b Guangxi Key Laboratory of Green Processing of Sugar Resources, College of Biological and Chemical Engineering, Guangxi University of Science and Technology, Liuzhou 545006, China

^c Jiangsu Province Hi-Tech Key Laboratory for Biomedical Research, Southeast University, Nanjing 211189, China

^d State Key Laboratory for the Chemistry and Molecular Engineering of Medicinal Resources, Collaborative Innovation Center For Guangxi Ethnic Medicine, School of Chemistry and Pharmaceutical Sciences of Guangxi Normal University, Guilin 541004, China

ARTICLE INFO

Keywords:

Platinum(IV) prodrugs
ER stress
Antitumor
Apoptosis
Chalcones

ABSTRACT

Platinum(II)-based chemotherapeutics are commonly used to treat various types of solid tumors, such as lung cancers. However, these compounds can cause serious side effects, including nephrotoxicity and ototoxicity, which affect the quality of life of patients. In our work, four novel dual target platinum(IV) complexes were designed and synthesized. In vitro results indicated that the title platinum(IV) complexes exhibited effective antitumor activities against the tested cancer cells and had lower toxicity and resistance factors than oxaliplatin and cisplatin. Further mechanistic experiments demonstrated that complex **11** accumulated in mitochondria and induced an elevation in ROS and an ER stress response via mitochondrial dysfunction. Notably, complex **11** significantly modulated the expression levels of proapoptosis proteins including cleaved-Caspase-3, Bax, and p53, and decreased the level of the prosurvival protein Bcl-2. Together, these results suggested that complex **11** might be a potential lead compound for future cancer therapy due to its potency and selectivity.

1. Introduction

Platinum(II) complexes (Fig. 1), including cisplatin, carboplatin and oxaliplatin, have been widely used as chemotherapeutics against many human solid tumors [1,2]. Despite the great achievements of platinum(II)-based anticancer drugs, their utilization in the clinic has been hampered by serious side effects and acquired drug resistance [3,4]. Therefore, extensive studies aiming to identify new prominent platinum candidates with enhanced anticancer activity but reduced toxicity and increased stability have been undertaken to overcome the inherent shortcomings of platinum(II) complexes.

In recent years, a vast number of studies have indicated that platinum(IV) complexes, which offer great therapeutic advantages, are promising for the development of the next generation of platinum drugs.

In contrast to platinum(II) drugs, platinum(IV) scaffolds exhibit oral availability, antitumor activity, and low toxicity [5–8]. Several outstanding complexes, including ormaplatin (also called tetraplatin), the highly water-soluble iproplatin, and the orally active satraplatin (JM216) have progressed onto clinical trials [9–12]. Notably, platinum(IV) complexes have two axial ligands, which provide the possibility of introducing active molecules with improved anticancer activity or targeting groups (for example, a cyclic RGD tripeptide, chlorotoxin, and biotin) to enhance functionality [13,14]. For example, in several over-expressed CLC-3 cancer cells, chlorotoxin (CTX)-functionalized platinum(IV) complexes, which can bind specifically to a chloride channel protein (CLC-3), can enhance intracellular uptake and subsequently induce better cytotoxicity than CTX and its platinum(II) complexes [14]. Moreover, platinum(IV) complexes are generally accepted to act as

* Corresponding authors at: State Key Laboratory for the Chemistry and Molecular Engineering of Medicinal Resources, Collaborative Innovation Center For Guangxi Ethnic Medicine, School of Chemistry and Pharmaceutical Sciences of Guangxi Normal University, Guilin 541004, China.

E-mail addresses: viphuangxc@126.com (X. Huang), wangxu504@126.com (X. Wang), whengshan@163.com (H. Wang).

¹ Co-first author: These authors contributed equally to this work.

<https://doi.org/10.1016/j.bioorg.2021.104741>

Received 13 October 2020; Received in revised form 30 January 2021; Accepted 8 February 2021

Available online 18 February 2021

0045-2068/© 2021 Elsevier Inc. All rights reserved.

prodrugs owing to reduction by intracellular reductants, such as glutathione or ascorbic acid, and high-molecular reducing agents, including metallothionein, that are usually present at high concentrations in tumor cells [15,16]. In addition, platinum(IV) complexes also tend to possess high stability because of their intrinsic kinetics [7]. Therefore, the exploration of novel platinum(IV) anticancer complexes, especially ones with improved therapeutic outcomes, that can overcome the drawbacks of platinum(II) drugs and possess unique action mechanisms has become an attractive topic in recent years.

Chalcone-based compounds that contain an α,β -unsaturated ketone moiety have been widely reported to display various biological activities, especially anticancer activities [17–19]. Many studies have recently demonstrated that natural or synthetic chalcone derivatives can act as novel tubulin polymerization inhibitors by inhibiting tubulin polymerization and combining with the colchicine binding site. Furthermore, chalcone-based derivatives have considerable potential antiproliferation effects against many types of solid tumors [20–22]. For example, the chalcone derivative Millepachine (**1a**, Fig. 2), a novel tubulin polymerization inhibitor isolated from *Millettia pachycarpa*, exhibits good anticancer activities against different human cancer cells [23]. Accordingly, as reported by Wang and co-workers, most Millepachine derivatives (such as **1b**, Fig. 2) present great potential in inhibiting tubulin polymerization and antiproliferative activities [24]. Interestingly, Schobert and co-workers reported that chalcone-based platinum(II) complexes also present potent antiproliferative activities and inhibit tubulin polymerization [25]. Thus, we imagined that incorporating a tubulin-targeted chalcone fragment into platinum(IV) complexes will be an effective strategy for developing novel platinum(IV) anticancer drugs. Therefore, in the present study, a series of chalcone-modified platinum(IV) compounds **8–11** were designed and prepared (Scheme 1). All of the platinum(IV) complexes were characterized via ^1H NMR, ^{13}C NMR, and HR-MS analysis. Finally, we investigated the *in vitro* antiproliferative activities and action mechanism of the compounds.

2. Results

2.1. Synthesis and characterization

The synthetic route to obtain title compounds **8–11** were described in Scheme 1. Chalcone **3** was prepared from 3,4,5-trimethoxyacetophenone (**1**) and isovanillin (**2**) in one step through Claisen-Schmidt condensation reaction according to the reported procedure [26]. In addition, the hydroxyalkyl functionalized chalcone analogues **4** and **5** were obtained by Williamson etherification of the compound **3** with succinic anhydride or glutaric anhydride in DMF in the presence of potassium carbonate at 50 °C for 2 h. The intermediate platinum(IV)

complexes **6** and **7** were obtained through the oxidative reaction of the oxaliplatin or DACHPt with *N*-chlorosuccinimide (NCS) in water according to a modified literature procedure [27,28]. Moreover, the target compounds **8–11** obtained by the formation of ester bond between compound **4** or **5** and **6** or **7** in the presence of TBTU/ Et_3N in DMF, and the target platinum(IV) complexes **8–11** were characterized by ^1H NMR, ^{13}C NMR spectra and ESI-MS spectroscopy as well as elemental analysis.

2.2. *In vitro* cytotoxicity of complexes **8–11**

The *in vitro* cytotoxicity of platinum(IV) complexes **8–11** were investigated in SK-OV-3 (ovary), HCT-116 (colon), HepG-2 (hepatoma) and MCF-7 (breast) and normal cells LO2 (Liver) with oxaliplatin, DACHPt, and compound **3** as reference controls using MTT assay. As depicted in Table 1, complexes **8–11** showed significant anticancer activities against all tested human tumor cells, with IC_{50} values ranging from 0.27 to 0.60 μM , which were significantly lower than that of oxaliplatin ($\text{IC}_{50} = 4.21 \sim 12.05 \mu\text{M}$) and DACHPt ($\text{IC}_{50} = 7.23 \sim 13.19 \mu\text{M}$). Besides, complexes **8–11** also exhibited lower toxicity toward normal cells (LO2) as compared with the oxaliplatin and DACHPt, respectively. Taken the toxicity of the Pt(IV) derivatives in cancer cells in consideration, complex **11** ($\text{IC}_{50} = 0.27 \sim 0.39 \mu\text{M}$) exhibited significantly more potent cytotoxicity against all tested human cancer cell lines than oxaliplatin ($\text{IC}_{50} = 4.21 \sim 12.05 \mu\text{M}$). Notably, complex **11** ($\text{IC}_{50} = 0.27 \pm 0.09 \mu\text{M}$), exhibited up to 37.8-fold and 2.7-fold increased cytotoxicity against HepG-2 cells than that of oxaliplatin ($\text{IC}_{50} = 10.20 \pm 1.02 \mu\text{M}$) and **3** ($0.75 \pm 0.12 \mu\text{M}$), while lower cytotoxicity against LO2 cells was found. A similar trend was also observed in other human cancer cells. Moreover, we also investigated the antiproliferative activities of combined group (Oxa + **3**, 1:1, n/n) against these cells mentioned above. As shown in Table 1, the combined group (Oxa + **3**) exerted great potential in anti-proliferative effects against the cancer cells tested in this manuscript, with IC_{50} values ranged from 0.41 to 0.83 μM , which was quite the same as that of compound **3**. However, it should be noticed that the combined group (Oxa + **3**) also appeared to be cytotoxic toward human normal cells (LO2) and shared poor tumor cell selectivity (SI was 1.4). Taken, all these results together, we believe that the anti-proliferative activity of complex **11** came from both components of oxaliplatin and compound **3** rather than each of them. In sum, these results suggested that the platinum(IV) derivatives of oxaliplatin, or DACHPt conjugated with **3** derivative ligand in the axial position can enhance cytotoxic activities together with decrease toxicity toward normal cells LO2.

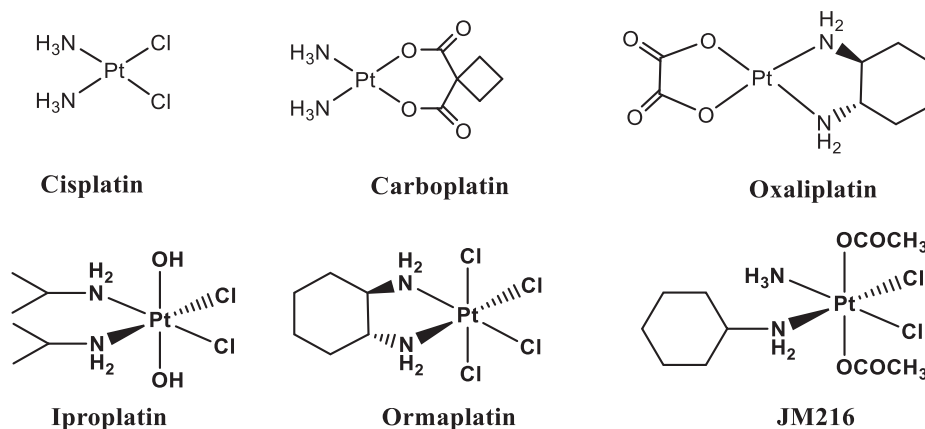


Fig. 1. FDA approved platinum(II) anticancer agents (etc., cisplatin, carboplatin and oxaliplatin), and platinum(IV) prodrugs in clinical trials (etc., iproplatin, ormaplatin and JM216).

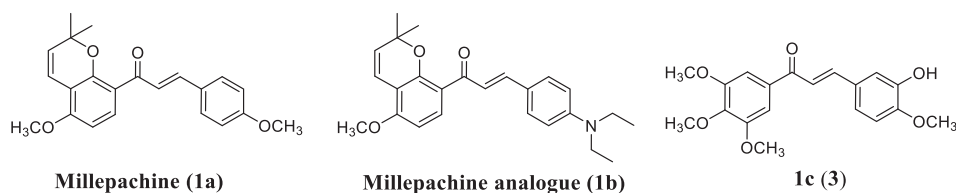
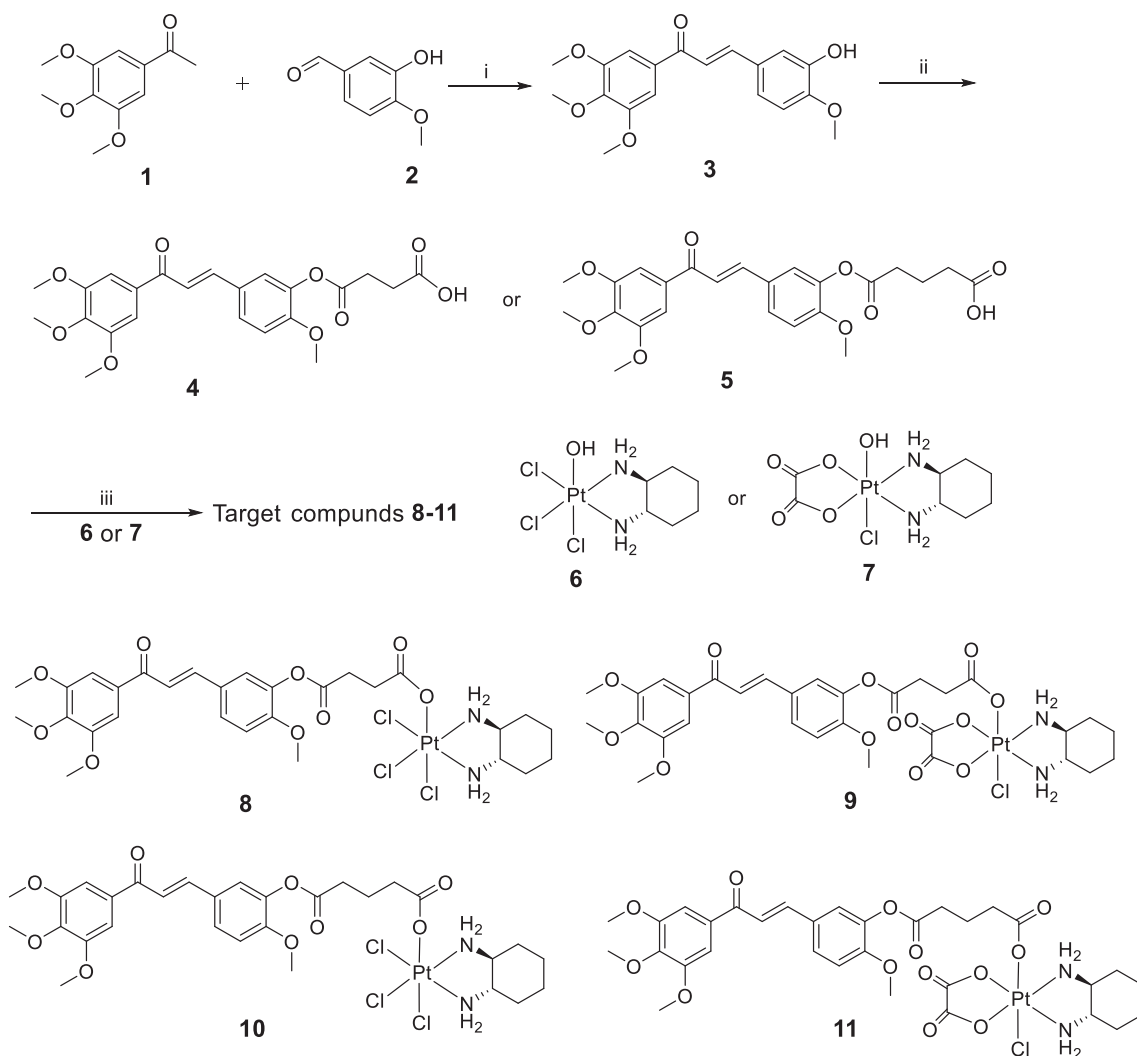


Fig. 2. Structures of chalcone analogues as potent inhibitors of tubulin polymerization.



Scheme 1. Synthetic pathway to target compounds 8-11. Reagents and conditions: (a) KOH (50% w/v aqueous solution), CH₃OH, 0 °C, overnight; (b) Succinic anhydride or glutaric anhydride, K₂CO₃, DMF, 50 °C.; (c) TBTU, Et₃N, DMF, 30 °C.

2.3. Anti-proliferative activity of complex 11 against drug-resistant cancer cells

It is generally accepted that acquired resistance is a major obstacle to drug therapy [3,5]. According to the above biological results, the cytotoxicity of complex 11 was further investigated in cisplatin-sensitive (A549 and SGC-7901) and cisplatin-resistant (A549/CDDP and SGC-7901/CDDP) cancer cell lines with cisplatin, oxaliplatin and DACHPT as controls using the MTT method. As shown in Table 2, complex 11 showed a more potent cytotoxic effect in A549, SGC-7901 and A549/CDDP, SGC-7901/CDDP cancer cells than that of cisplatin, and the cytotoxicity activity of complex 11 was not obviously changed against cisplatin resistant cells A549/CDDP and SGC-7901/CDDP, with IC₅₀ value of 0.31 ± 0.09 and 0.71 ± 0.18 μM as compared with the

commercial drug cisplatin (35.05 ± 1.39 and 26.81 ± 1.73 μM), respectively. Notably, the complex 11 exhibited a lower RF (RF = 1.3 and 1.2) compared to the cisplatin (RF = 7.7 and 7.6, respectively) against two cisplatin resistant cells A549/CDDP and SGC-7901/CDDP (Table 2).

The great potency in anti-proliferative activities against cisplatin resistant A549/CDDP cells may raise a question that whether the incubation time affected the intrinsic anti-tumor effects. With this doubt in mind, we performed *in vitro* cytotoxicity assays of 24 h, 48 h and detected the IC₅₀ values against A549 and A549/CDDP cells. As summarized in Table S1, significantly decreased anti-proliferative effects against A549 or A549/CDDP cells were displayed after 24 h co-incubation with various tested compound. Compound 11 showed little cytotoxic effect in both A549 and A549/CDDP cells (IC₅₀ values were

Table 1
Cytotoxic effects of complexes **8–11** on human cancer and normal cell lines.

Comps.	IC ₅₀ (μM) ^d					
	SK-OV-3	HCT-116	HepG-2	MCF-7	LO2	SI ^e
8	0.55 ± 0.08	0.53 ± 0.03	0.39 ± 0.11	0.56 ± 0.13	10.95 ± 1.42	28.1
9	0.60 ± 0.11	0.32 ± 0.05	0.34 ± 0.05	0.48 ± 0.09	11.31 ± 1.51	33.3
10	0.47 ± 0.07	0.45 ± 0.12	0.41 ± 0.14	0.43 ± 0.10	13.05 ± 1.49	31.8
11	0.39 ± 0.06	0.29 ± 0.07	0.27 ± 0.09	0.33 ± 0.08	12.07 ± 1.63	44.7
3	0.81 ± 0.13	0.87 ± 0.21	0.75 ± 0.12	0.97 ± 0.16	4.52 ± 0.58	6.0
Oxa + 3 ^a	0.41 ± 0.08	0.54 ± 0.10	0.72 ± 0.09	0.83 ± 0.14	1.03 ± 0.06	1.4
DACHPt ^b	9.48 ± 0.71	7.23 ± 0.87	12.07 ± 1.23	13.19 ± 1.71	6.35 ± 1.13	0.5
Oxa ^c	12.05 ± 0.93	4.21 ± 0.65	10.20 ± 1.02	11.26 ± 1.22	8.06 ± 1.05	0.8

^a The combined group of oxaliplatin and **3** (1:1, n/n).

^b Dichloro(1R,2R-diaminocyclohexane) platinum(II).

^c Oxaliplatin.

^d In vitro cytotoxicity was determined by MTT assay upon incubation of the live cells with the compounds for 72 h.

^e Selectivity Index = IC₅₀(LO2)/IC₅₀(HepG-2). Mean values based on three independent experiments.

Table 2
Anti-proliferative activities of optimal complex **11** on the cisplatin-resistant cells A549 and SGC-7901.

Comps.	IC ₅₀ (μM) ^d					
	A549	A549/CDDP	RF ^e	SGC-7901	SGC-7901/CDDP	RF ^e
11	0.23 ± 0.07	0.31 ± 0.09	1.3	0.57 ± 0.16	0.71 ± 0.18	1.2
3	0.70 ± 0.10	1.25 ± 0.28	1.8	1.21 ± 0.08	2.05 ± 0.72	1.7
CDDP ^a	4.55 ± 0.82	35.05 ± 1.39	7.7	3.53 ± 0.08	26.81 ± 1.73	7.6
DACHPt ^b	10.43 ± 1.46	31.30 ± 2.31	3.0	10.38 ± 1.02	27.05 ± 1.89	2.6
Oxa ^c	9.05 ± 1.46	25.83 ± 1.84	2.9	9.25 ± 0.88	25.36 ± 1.55	2.7

^a Cisplatin.

^b Dichloro(1R,2R-diaminocyclohexane)platinum(II).

^c Oxaliplatin.

^d In vitro cytotoxicity was determined by MTT assay upon incubation of the live cells with the compounds for 72 h.

^e Resistant factor = (IC₅₀ human resistance cells)/(IC₅₀ human cancer sensitive cells).

5.21 and 6.08 μM), which were almost the same as that of **3** (IC₅₀ were 7.03 and 9.12 μM, respectively). However, when the incubation time was extended to 48 h, sharply decrease in IC₅₀ values were found, especially for **11** in A549 or A549/CDDP cells. Nevertheless, the anti-proliferative effects of **3**, **11** or both against A549 and A549/CDDP cells were weaker than that of 72 h (Table S1).

2.4. The release of compound **5** and stability of compound **11** in various conditions

The stability of compound **11** in various conditions was monitored via reversed phase high performance liquid chromatography (HPLC). Briefly, solutions of **11** (50 μM) in PBS (150 mM) and acetonitrile (10 mL, 9.5:0.5, V/V) and ascorbic acid (500 μM) in PBS (pH = 7.4, 150 mM) were prepared, using solutions of oxaliplatin (50 μM) and compound **5**

(50 μM) as controls to match the peaks during the assays. As illustrated in Fig. S1D and S1E, compound existed stable in physiological environment of a PBS solution (pH = 7.4) in 72 h. However, upon mixing with the same volume of ascorbic acid in dark, compound **11** gradually decomposed, illustrating as the decreased peaks of **11** in HPLC spectra along with the extension of incubation time (Fig. S1C and S1F). Interestingly, the decomposition of **11** led to another increased peak, which was right at the position of compound **5**, indicating that compound was reduced to compound **5** and the reaction completed in 7 h. It should be note that oxaliplatin appeared at the same position as that of ascorbic acid in HPLC spectra (Fig. S1A and S1B) and only slight increased peaks occurred at the end of the reduction (5–7 h in Fig. S1F). Taken together, all the results revealed that complex **11** acted as a prodrug and released corresponding oxaliplatin and compound **11** under the reduction of ascorbic acid. Subsequently, we investigated the stability of compound **11** (50 μM) in other conditions, including DMF (containing PBS 50%), DMEM and DMEM + FBS and monitored at different time points of 0 h, 6 h, 24 h, 48 h and 72 h. As shown in Fig. S1G–S1I, compound **11** maintained stable in 72 h co-incubation of these solutions indicated except for negligible decomposition in DMEM + FBS in 72 h (Fig. S1I).

Furthermore, we also investigated the intracellular existence form of compound **11** via the same HPLC methods. Briefly, A549 cells were treated with compound **11** (10 μM) for 24 h and lysate was used for HPLC analysis. The calibration curve of compound **3** was shown in Fig. S2A while the HPLC spectra of lysate indicated in Fig. S2B. As shown in Fig. S2B, we found four target peaks, including oxaliplatin (2.019 min), compound **11** (6.951 min), compound **3** (8.492 min) and compound **5** (9.078 min). Moreover, higher concentration of 1.53 μM (calculated by calibration curve of compound **3**) were recorded than negligible compound **5**, indicating that the intracellular compound **11** was reduced and thereafter mainly produced compound **3** (Fig. S2B).

2.5. Cell uptake and possible pathway of intracellular uptake

Many studies demonstrated that the cellular uptake is recognized as an important factor influencing anti-proliferative performance of platinum compounds [29]. Owing to the complex **11** exhibited more potent cytotoxicity in A549 cells, thus it was used in subsequent experiments investigating the mechanism of anticancer activity in the human lung cancer cells A549. Thus, in order to further evaluate the cellular uptake properties of complex **11**, here we used ICP-MS to detect the levels of the complex **11** in human lung cancer cells A549. As shown in Fig. 3, after the cells were treated with complex **11** (5 and 10 μM) and oxaliplatin (5 and 10 μM) for 12 h, the platinum(IV) complex **11** accumulate at 1.9 ~ 2.4 times higher levels in whole cells than that of the positive drug oxaliplatin at the indicate concentrations, indicating platinum(IV) complex **11** exhibited higher platinum accumulation in A549 cells than that of the reference drug oxaliplatin, which is probably attributed to the high lipophilicity of complex **11**. Generally, small molecules enter cells by passive diffusion whereas macromolecules through energy-dependent endocytosis [29]. Therefore, in order to investigate the whether the internalization of **11** was energy-dependent, the cells were pre-treated with sodium azide (10 mM) (which depletes intracellular ATP) for 4 h followed with another 12 h co-incubation under the same condition [29]. As shown in Fig. 3, in the presence of sodium azide, intracellular uptake of complex **11** (5 μM) changed little while that of **11** (10 μM)-treated group was 290 ng/10⁶ cells, which was significantly lower than 363 ng/10⁶ cells of untreated group. Interestingly, with 4 h pretreatment of sodium azide, the amount of intracellular oxaliplatin was significantly decreased as compared with untreated group. Taken all these results, we believed that **11** entered cells mainly by passive diffusion at lower concentration, but which was significantly affected in an energy-dependent way at high concentration.

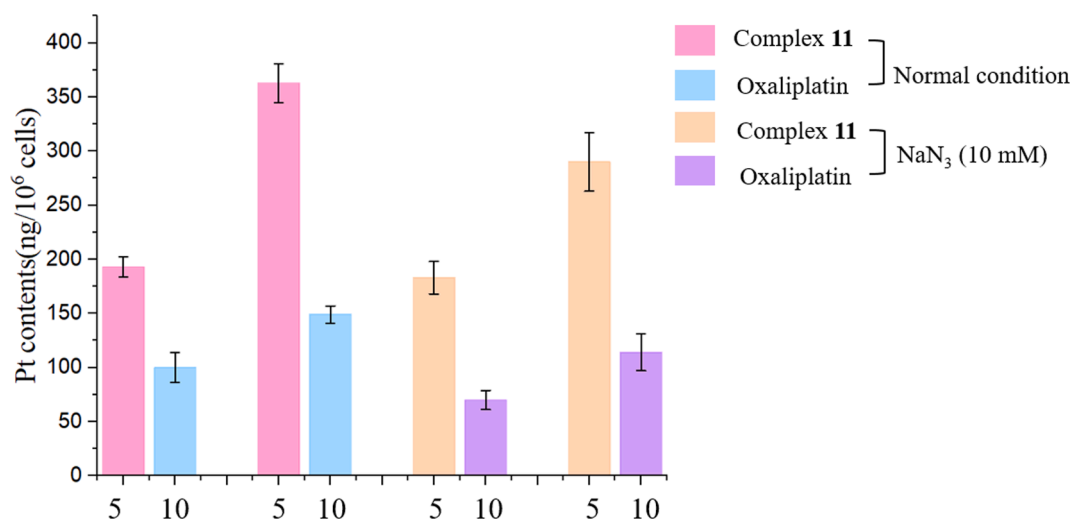


Fig. 3. Cellular uptake of the platinum(IV) complex 11 (5 and 10 μM) and oxaliplatin (5 and 10 μM) in A549 cells in the absence or presence of sodium azide (10 mM). The results were obtained and analyzed with ICP-MS and showed as one of three independent experiments.

2.6. Analysis of immunofluorescence staining

Microtubules played a crucial role in a variety of cellular process,

especially for mitosis. Thus, it was of great significance to disturb the microtubule dynamics in cancer cells to block mitosis or induce apoptosis [21]. Besides, our previous reports explained that a structure

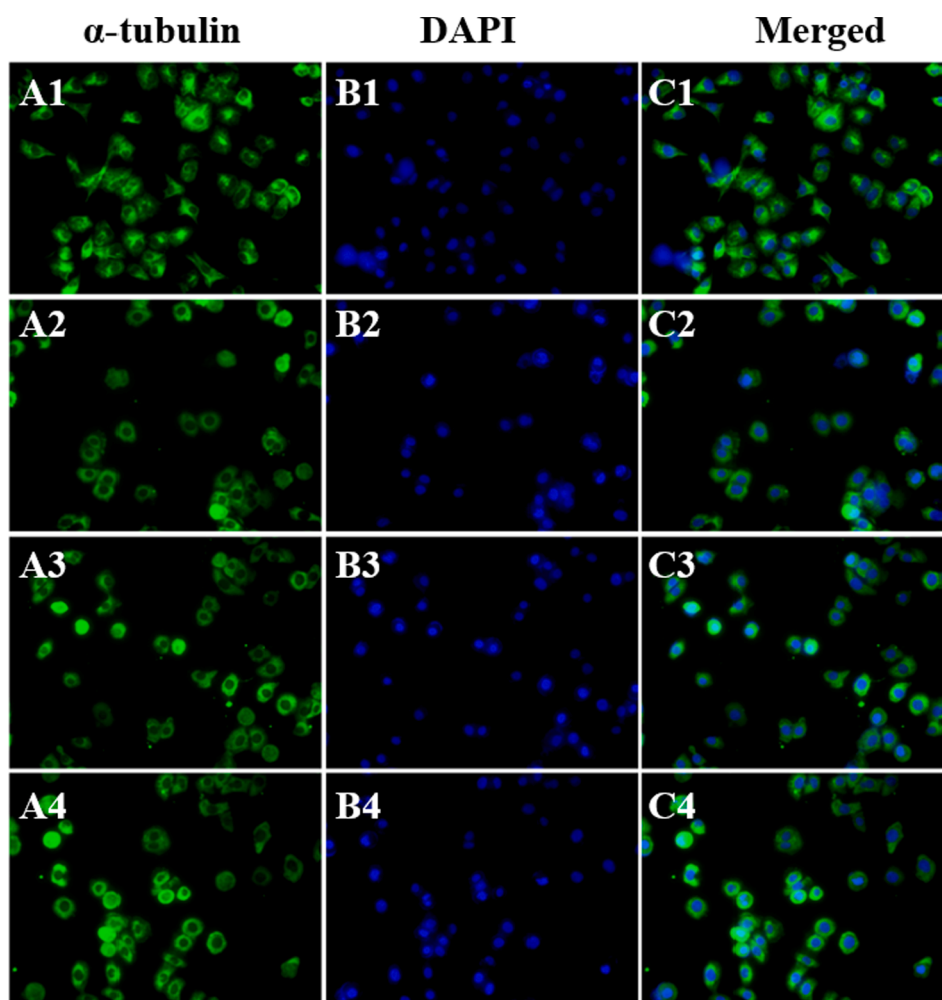


Fig. 4. Effects of 11 on microtubules network. A549 cells were untreated (A1-C1), incubated with 3 (A2-C2, 10 μM), incubated with 11 (A3-C3, 5 μM), incubated with 11 (A4-C4, 10 μM) for 24 h, fixed and visualized by treatment α-tubulin monoantibody and IgG FITC conjugated antibody. DAPI was used as track the cells. The results were shown as one of three independent experiments.

of chalcone obtained inhibitory activities on microtubules polymerization [30]. Therefore, for the purpose to confirm the mechanism of the action of target complex **11**, immunofluorescence assays on microtubules polymerization were performed. As shown in Fig. 4A1-C1, the microtubule structures in A549 cells of untreated-group were slim and fibrous, appearing from nuclear region to the plasma membrane. However, when treated with **11**, the tubulin network was altered and condensed around the nucleus. Moreover, in the presence of **11** (10 μM) the spindle microtubules turned aberrant multipolar or irregular or complete absent (Fig. 4A4-C4), which illustrated that complex **11** efficiently inhibited microtubules polymerization and thereafter block mitosis and finally induced apoptosis. Not surprisingly, compound **3**, a ligand of **11**, shared the same inhibitory effects on microtubules polymerization (Fig. 4A3-C3).

2.7. Cell cycle analysis

The anti-proliferation tests and apoptosis tests showed that **11** obtained the best potential in inducing apoptosis in A549 cells. Therefore, to investigate the effects on cycle, A549 cells were co-incubated with **11** (2.5 and 5 μM) for 24 h, fixed with ice-cold ethanol at $-20\text{ }^{\circ}\text{C}$ overnight, stained with PI and subjected to flow cytometry assays. Similarly, vehicle (DMF), oxaliplatin (10 μM), **3** (5 μM), combined group (oxaliplatin, 10 μM , **3**, 5 μM) were used as controls. As revealed in Fig. 5, oxaliplatin-treated A549 cells were mainly arrested at S phase as comparison with untreated cells (S phases, 36.24%), while A549 cells treated with compound **3** were mainly arrested at G2/M phase (G2/M phase, 23.45%). Moreover, cells incubated with **11** (2.5 and 5 μM) for 24 h were mainly arrested at G2/M phase in a dose-dependent manner with the percentage increased from 28.30% to 58.09% and could not escape this phase (Fig. 5). Interestingly, when A549 cells were treated with combined group (oxaliplatin, 10 μM , **3**, 5 μM), 50.44% of cells were arrested at G2/M phase, which was not distinctive to that of **11**-treat

but was obviously different from that of oxaliplatin-treated cells. In sum, complex **11** induced A549 cells G2/M phase arrestment in a dose-dependent manner which contributed to apoptosis and anti-proliferation in cancers.

2.8. Complex **11** induced apoptosis in A549 cells

The perfect anti-proliferation activity against A549 cells *in vitro* motivated us to investigate whether the inhibitory effects of **11** on A549 cells were due to the enhanced apoptosis. Therefore, A549 cells were seeded into 6-well plates and incubated with various compounds of oxaliplatin (10 μM), **3** (5 μM), combined group (oxaliplatin, 10 μM , **3**, 5 μM) and **11** (2.5 and 5 μM), respectively. Similarly, cells seeded in complete culture medium and were treated with DMF as controls. After 24 h co-incubation, the cells were collected and double-stained with Annexin V-FITC and propidium iodide (PI) and subjected to flow cytometry assays. The results in Fig. 6 showed that oxaliplatin (10 μM) or compound **3** (5 μM) induced apoptosis in 13.95% or 16.72% in A549 cells. However, when co-treatment with **3** (5 μM) and oxaliplatin (10 μM) the percentage of A549 cells in apoptosis increased to 39.43%, which revealed that the combined usage of **3** and oxaliplatin more easily contribute to apoptosis than one of **3** and oxaliplatin. More importantly, when A549 cells were exposed to **11** for 24 h, the cells in apoptotic state increased from 31.95% to 42.87% in a dose-dependent manner. Altogether, the results in apoptosis data illustrated that **11** was more potential in inducing apoptosis in A549 cells than **3** or **11** or both at the same concentration.

2.9. Mitochondrial membrane potential (MMP) assays

To further investigate whether apoptosis in A549 cells induced by **11** was executed by the collapse of mitochondrial membrane potential (MMP). Fluorescent mitochondrial dye, 5,5,6,6'-tetrachloro-1,1,3,3-

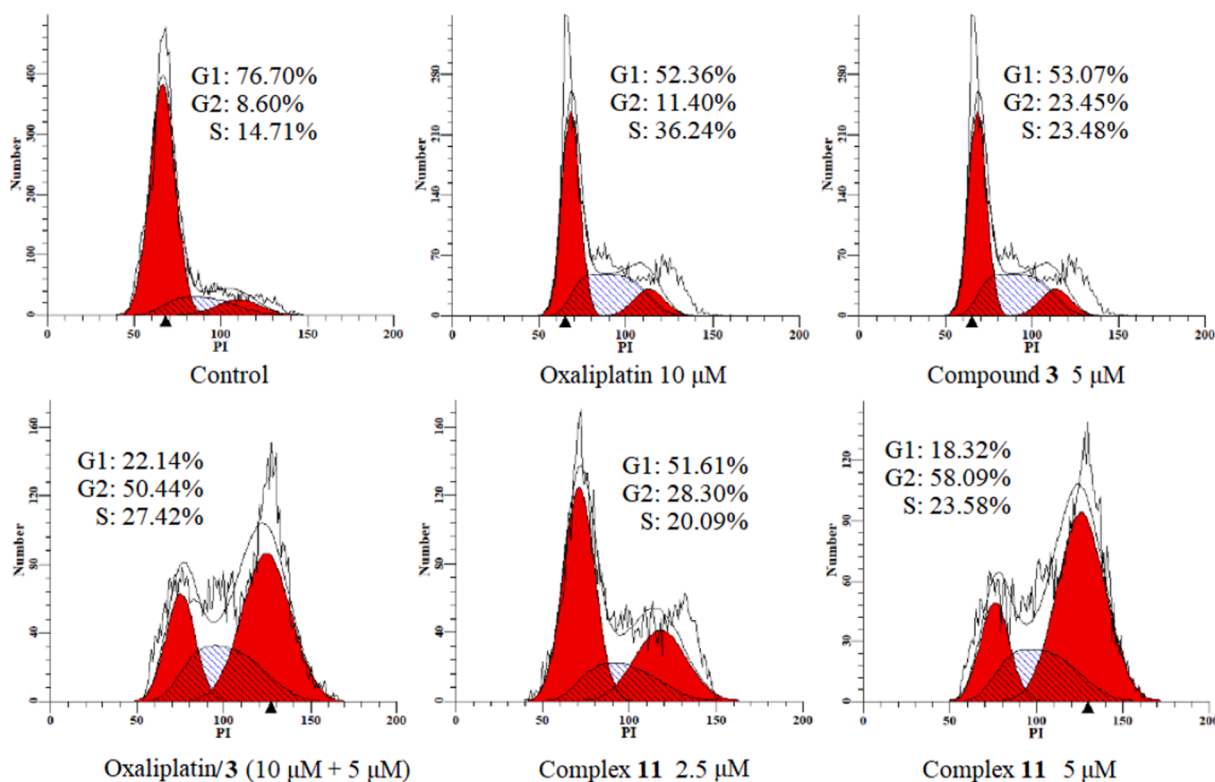


Fig. 5. Cell cycle arrest assays induced by **11**. A549 cells were incubated with vehicle (DMF), oxaliplatin (10 μM), **3** (5 μM), combined group (oxaliplatin, 10 μM , **3**, 5 μM), **11** (2.5 and 5 μM) for 24 h, collected and fixed with ice-cold ethanol at $-20\text{ }^{\circ}\text{C}$ overnight. The cells were stained with PI, collected and subjected to flow cytometry. The results were shown as one of three independent experiments.

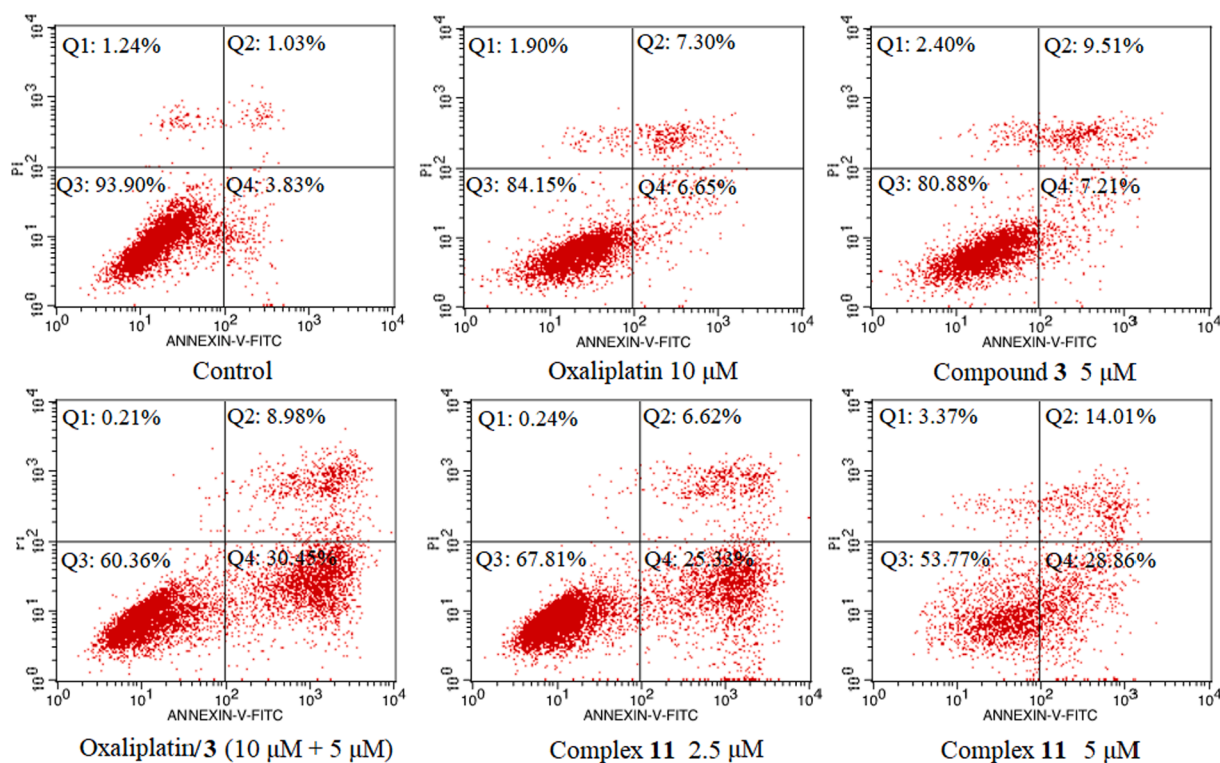


Fig. 6. Apoptosis assays induced by 11. A549 cells were co-incubated with control (DMF), oxaliplatin (10 μ M), 3 (2.5 μ M), combined group (oxaliplatin, 10 μ M, 3, 2.5 μ M), 11 (2.5 and 5 μ M) for 24 h, collected and stained with Annexin-V and PI. Q1, Q2, Q3, and Q4 represent four different cell states: necrotic cells, late apoptotic cells, living cells and apoptotic cells, respectively. The results were obtained and analyzed with flow cytometry and showed as one of three independent experiments.

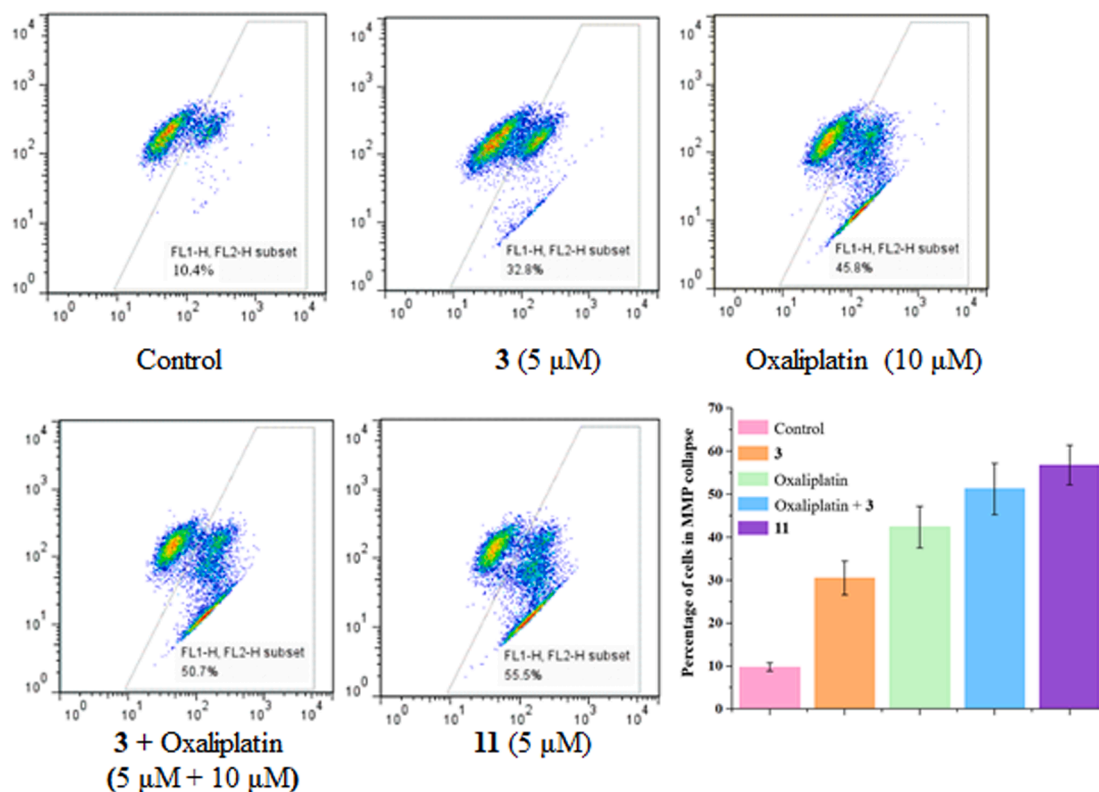


Fig. 7. Complex 11 induced loss of mitochondrial membrane potential in A549 cells. A549 cells were incubated with various compounds of vehicle (DMF), 3 (5 μ M), oxaliplatin (10 μ M), combined group (oxaliplatin, 10 μ M, 3, 5 μ M) and 11 (5 μ M) for 24 h. After that, the cells harvested for JC-1 staining and analyzed via flow cytometry. The results were presented as one of three independent experiments.

tetraethyl-imidacarbocyanine (JC-1) was used to detect the transition of MMP. Generally, A549 cells were incubated with pretreated with vehicle (DMF), oxaliplatin (10 μM), **3** (5 μM), combined group (3, 5 μM , oxaliplatin, 10 μM), and **11** (2.5 and 5 μM) for 24 h, washed with cold PBS, and collected for JC-1 staining. Generally, in healthy cells, the dye easily entered in mitochondria and aggregated in red fluorescence, while the MMP collapsed in apoptosis cells, the dye cannot accumulate in mitochondria and dispersed into cytoplasm in green fluorescence. In Fig. S3 A1-C1, the mitochondria in healthy A549 cells of control group were stained in red fluorescence while the mitochondria in **3**-treated or oxaliplatin-treated were shown in more green fluorescence than red fluorescence (Fig. S3 A2-D3), which clearly explained that **3** and oxaliplatin decrease MMP in A549 cells. It was worth noting that the combined group of **3** (5 μM) and oxaliplatin (10 μM) can only partly induced MMP collapse with red fluorescence remaining in A549 cells. Interestingly, **11** induced concentration-dependent collapse of mitochondrial membrane potential and seem to disturb all of the mitochondrial transition in A549 cells in concentration of 10 μM , leading to the randomly distribution of green JC-1 monomer in cytoplasm. Herein, we performed quantitative analysis via flow cytometry instrument to investigate the changes induced by these compounds indicated above. As shown in Fig. 7, 32.8 percent of cells were in the status of MMP collapse in **3** (5 μM) treated group whereas that of oxaliplatin (10 μM) treated group was increased to 45.8%. However, after 24 h co-treatment with **11** (5 μM), the population rose to 55.5% which was slightly better than 50.7% of combined group (oxaliplatin + **3**, 10 + 5 μM). In sum, the sharply decreased red fluorescence intensity induced by **11** clearly suggested that **11** disturbed the function of mitochondria in A549 cells and thereafter induced cytotoxicity in A549 cells.

2.10. Complex **11** triggered reactive oxygen species (ROS) generation

Previously, platinum(IV) complexes were reported to disturb redox balance in cancer cells, leading to the accumulation of intracellular ROS and apoptosis [31-33]. To investigate whether the inhibitory effects of **11** on A549 cells cellular proliferation, intracellular ROS accumulation was detected. Briefly, A549 cells were independently treated in triplicate with various compounds of **3** (5 μM), oxaliplatin (10 μM), combined group (3, 5 μM , oxaliplatin, 10 μM), and **11** (2.5 and 5 μM). After 24 h-coincubation with these compounds mentioned above, the cells were washed with cold PBS, collected and stained with DCFH-DA (Beyotime) to record and analyze the laser confocal microscope. As shown in Fig. S4 A2-C3, treatment with compound **3** (5 μM) or oxaliplatin (10 μM) only

induced moderate intracellular ROS accumulation in A549 cells. However, a large number of A549 cells were in ROS-overexpression status when treated with combined compounds of **3** (5 μM) and **11** (10 μM) (Fig. S4 A4-C4) which illustrated that **3** and **11** in some degree co-effected the accumulation of ROS in A549 cells. More interestingly, when treatment with **11** significantly and rapidly increased ROS levels were induced in almost all of A549 cells (Fig. S4 A5-C6). It was worth noting that **11** in low concentration (2.5 μM) was more preferably induced ROS accumulation than that of **3** or oxaliplatin or both (Fig. S4). Besides we also detected the ROS accumulation in A549 cells after 24 h incubation with various compounds indicated above. As illustrated in Fig. 8, moderate ROS accumulation was induced in **3** (5 μM) treated or oxaliplatin (10 μM) treated group. However, after exposure to complex **11** (5 μM) for 24 h intracellular ROS level was significantly elevated, which was more than two times of that in the combined group (oxaliplatin + **3**, 10 + 5 μM). Taken all these results together, we believed that complex was an efficient ROS inducer for intracellular ROS accumulation in cancer cells.

Moreover, many studies demonstrated that most of metal anticancer drugs could be ability to affect endoplasmic reticulum (ER) stress, which is an important factor in drug efficacy [33,34]. On the other hand, the simultaneous presence of promoted the accumulation of intracellular ROS and resulted ER stress can effectively induce the death of the tumor cells. In order to further investigate if complex **11** induce ER stress, the expression of three crucial ER stress markers, such as CHOP, p-eIF2 α and p-PERK was explored using western blotting assay. As depicted in Fig. 9A and B, it was observed that complex **11** significantly promoted the accumulation of these three proteins including CHOP, p-eIF2 α and p-PERK, indicating that the complex **11** may promote intracellular ROS production and induce an ER stress response ultimately leading to the death of A549 cells.

2.11. Complex **11**-induced apoptotic pathways

The Bcl-2 family proteins, such as pro-apoptosis protein Bax and pro-survival protein Bcl-2, are critical regulators of cell apoptosis [35,36], therefore we further investigated the apoptosis-associated protein alterations, the expression of Bax and Bcl-2 were analyzed. As shown in Fig. 9A, after treatment with oxaliplatin and complex **11**, the level of pro-apoptotic protein Bax was significantly up-regulated, and the anti-apoptotic protein Bcl-2 was down-regulated significantly. Increasing evidence has indicated that the p53 protein, as a crucial molecule in DNA damage repair and a cancer suppressor protein, which is involved

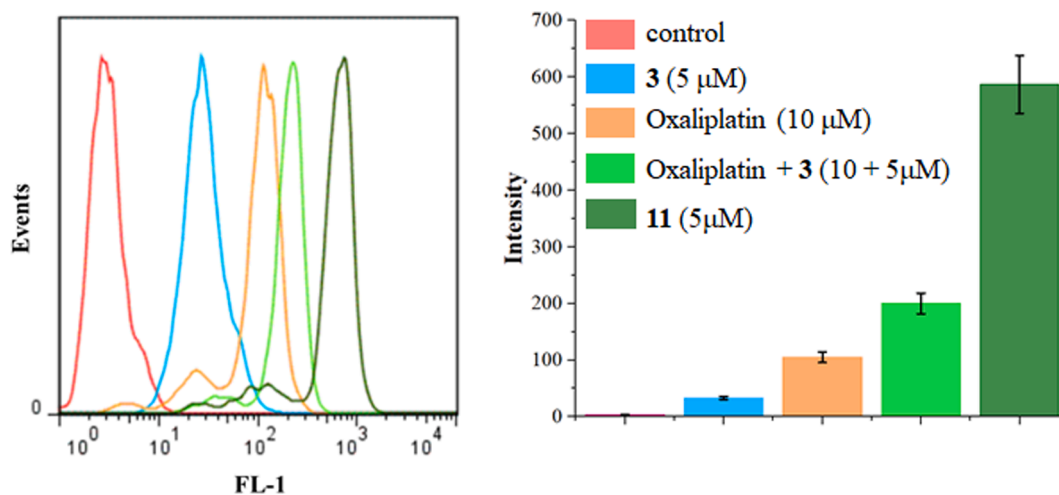


Fig. 8. Intracellular ROS accumulation assays induced by **11**. A549 cells were incubated with various compounds of vehicle (DMF), **3** (5 μM), oxaliplatin (10 μM), combined group (oxaliplatin, 10 μM , **3**, 5 μM) and **11** (5 μM) for 24 h. After that, the cells harvested for DCFH-DA staining and analyzed via flow cytometry. The results were presented as one of three independent experiments. (Excitation wavelength, 505 nm; Emission wavelength, 535 nm).

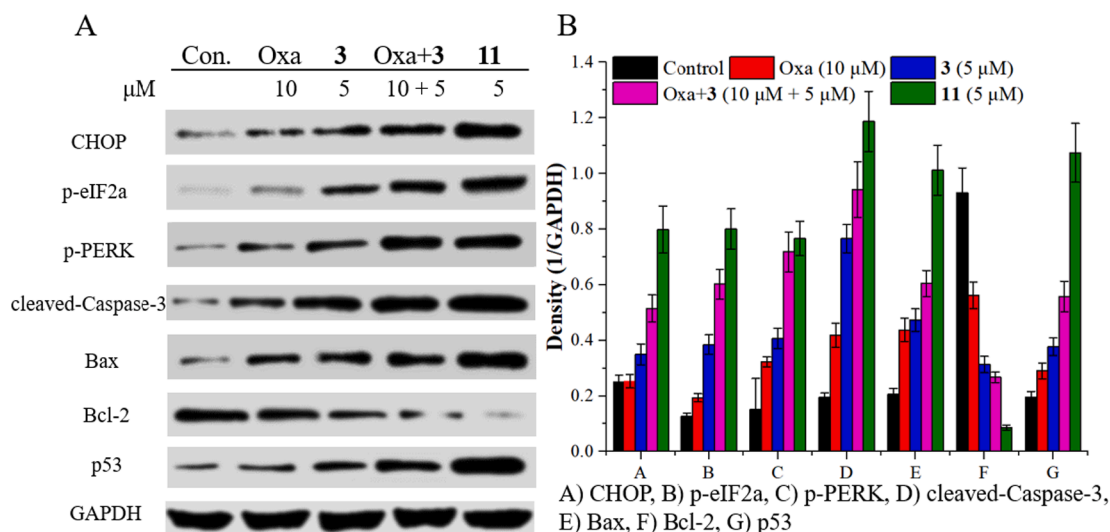


Fig. 9. The effects of complex **11** on the apoptosis-related protein. A549 cells of 24 h incubation with complex **11** (5 μM) or oxaliplatin (10 μM) were collected for western blotting assays. (A) Representative western blots in complex **11** treated A549 cells. (B) Percentage expression levels of CHOP, phosphor-eIF2a (p-eIF2a), phosphor-PERK (p-PERK), Bax, Bcl-2, cleaved-Caspase-3 and p53. The GAPDH was used as internal control and the percentage values are normalized with GAPDH.

in a multitude of biological processes (such as cell cycle arrest, apoptosis and autophagy, respectively) [37]. As depicted in Fig. 9A, treatment with complex **11** (5 μM) resulted in higher expression of the p53 protein, a marker of DNA damage, than that of combined group (oxaliplatin + **3**, 10 + 5 μM) though similar anti-proliferative activities exerted *in vitro*. Moreover, it is well known that the cleaved-Caspase-3 protein has been considered as an important effector of tumor cell apoptosis, and identified to be activated in response to chemotherapy drugs [38,39]. Therefore, we also investigated the expression level of cleaved-Caspase-3 by means of western blotting assay. As depicted in Fig. 9A, the expression level of cleaved-Caspase-3 protein was significantly up-regulated by complex **11**, oxaliplatin and combined group (Oxa + **3**) at the indicated concentrations compared to the untreated control cells (Fig. 9B), whereas the expression of cleaved-Caspase-3 protein was markedly up-regulated in contrast to that of the positive drug oxaliplatin.

3. Discussion

Cisplatin and its analogues, such as carboplatin and oxaliplatin, are widely used as first-line treatments in many therapeutic schemes [40]. However, their further improvement is urgently needed owing to their innate or acquired drug resistance and serious side effects. Currently, drug combination strategies based on multiple drugs with different mechanisms of action are regarded as effective approaches for overcoming the limitations of single-drug chemotherapy [41]. Given that platinum(IV) complexes are promising tools for designing multimodulatory drugs, we constructed four novel platinum(IV) prodrugs (**8–11**) based on tubulin polymerization inhibitor agents (chalcone derivatives) and oxaliplatin or DACHPt. As shown in Tables 1 and 2, platinum(IV) complexes **8–11** not only exhibited great potential in inhibiting the proliferation of cisplatin-sensitive (SK-OV-3, HCT-116, HepG-2, and MCF-7) and cisplatin-resistant (A549) cells but showed improved selectivity indexes for human normal cells (LO2). Notably, the target complex **11** also reversed cisplatin resistance in A549 cells, whereas the combined group (Oxa + **3**) showed potential cytotoxicity against normal human cells (LO2) with the SI value of 1.4. In contrast to the traditional multidrug combination used to combat resistance, complex **11** was a single compound that contained two drugs with the same pharmacokinetics that are easy to control. Furthermore, unlike oxaliplatin, **11** entered cells mainly via passive diffusion at low concentrations but was significantly affected in an energy-dependent manner at high

concentrations. Interestingly, as shown in Fig. S11, complex **11** maintained its stability in the physiological environment (pH = 7.4, DMEM, DMEM + FBS) but was efficiently reduced into oxaliplatin and compound **5** by ascorbic acid (Fig. S2B). Therefore, this complex could serve as a multifunctional antineoplastic agent to combat cancer cells, especially cisplatin-resistant cancer cells.

Additionally, as shown in Figs. 3 and 4, complex **11** could significantly improve the level of cellular uptake and efficiently inhibit microtubule polymerization. Traditionally, the antineoplastic mechanisms of platinum drugs have been proven to be the induction of DNA damage and the subsequent induction of apoptosis in cancer cells. As shown in Figs. 5 and 6, complex **11** significantly arrested the cell cycle at the G2/M phases and induced cell apoptosis. In addition, complex **11** enhanced the expression levels of proapoptosis proteins (such as Bax, cleaved-Caspase-3, and p53) and simultaneously suppressed the levels of the prosurvival protein Bcl-2 (Fig. 9). Previous studies have shown that the mitochondria play a major role in regulating cellular functions, and a decrement in MMP has been implicated as an early event in apoptotic cells [34]. Moreover, the death-inducing capacity of anti-tumor agents has been related to ROS production. As shown in Figs. 7 and 8, complex **11** significantly induced MMP collapse, mitochondrial dysfunction, and intracellular ROS accumulation. Additionally, the capability of chemotherapeutic drugs to affect ER stress is an important element in drug efficacy. Through further studies, we found that the expression levels of proteins, including CHOP, p-eIF2a, and p-PERK, had all increased (Fig. 9) after the incubation of A549 cells with complex **11**. This result indicated ER stress. Taken together, these results indicated that complex **11** disrupted mitochondrial membrane potential balance, induced intracellular ROS accumulation, and finally activated mitochondrion-dependent and ER-stress-mediated apoptosis pathways. These obvious differences might originate from the introduction of a chalcone derivative, which caused complex **11** inherit the advantages of chalcone and oxaliplatin to efficiently inhibit the proliferation of cancer cells at multiple levels of pathological mechanisms. All the results indicated that this novel series of dual-target platinum(IV) complexes showed low toxicities and enhanced the antineoplastic effects of oxaliplatin, especially its effects against cisplatin-resistant cancer cells.

4. Conclusions

Cisplatin and its analogues carboplatin and oxaliplatin are commonly used in chemotherapy for various human solid tumors, such

as lung cancers. However, high doses of these platinum(II)-based anticancer agents cause serious side effects, such as nephrotoxicity and ototoxicity, that affect the quality of life of patients. Here, we designed and synthesized four novel dual-target chalcone platinum(IV) complexes. We also explored their capability to be taken up by cancer cells and their antiproliferative activity in detail. The results of *in vitro* experiments demonstrated that the title complexes **8–11** showed more potent antiproliferative activity than platinum(II) drugs against the tested human cancer cell lines, including cisplatin-resistant cells (A549/CDDP). Among them, complex **11** displayed great anticancer activity against the tested cancer cells and reduced toxicity to normal LO2 liver cells. Moreover, complex **11** significantly induced G2/M stage arrest and DNA damage, inhibited microtubule polymerization, and triggered apoptosis in A549 cells. Notably, mechanistic experiment results indicated that complex **11** could cause mitochondrial dysfunction, generate significant levels of ROS, and further induce ER stress. Thus, these results indicated that complex **11** could induce cell death mainly through mitochondrial dysfunction and a ROS-mediated ER stress pathway. Interestingly, complex **11** had no cross-resistance with cisplatin owing to its dual target mechanisms of action.

5. Experimental section

All chemicals and solvents were analytical reagent grade and commercially available, and the column chromatography was performed using silica gel (200–300 mesh). The elemental analyses of C, H, and N used a Vario MICRO CHNOS elemental analyzer (Elementary), and ^1H NMR and ^{13}C NMR spectra were recorded in CDCl_3 or $\text{DMSO-}d_6$ with a Bruker 400 or 600 MHz NMR spectrometer, and the mass spectra were measured on an Agilent 6224 TOF LC/MS instrument.

5.1. General procedure for the preparation of compounds

5.1.1. (*E*)-3-(3-hydroxy-4-methoxyphenyl)-1-(3,4,5-trimethoxyphenyl)prop-2-en-1-one (**3**)

Compounds **1** (15.0 mmol) and **2** (15.0 mmol) was dissolved in methanol (30 mL) and cooled to ice-water, and then the 50% KOH (10 mL, aq) added to dropwise to the solution, respectively, and the solution was stirred at the same temperature for overnight. After completion of reaction, adjusted to pH = 1 ~ 2 with 4 N HCl, and washed with CH_2Cl_2 . The organic phase was dried with anhydrous Na_2SO_4 , and the resulting crude product was purified by silica gel column chromatography with $\text{CH}_3\text{OH}/\text{CH}_2\text{Cl}_2$ to obtain the final product **3** (3.4 g, 65.9%) as a yield solid. ^1H NMR (600 MHz, $\text{DMSO-}d_6$) δ 9.16 (s, 1H), 7.71 (d, $J = 15.4$ Hz, 1H), 7.63 (d, $J = 15.4$ Hz, 1H), 7.40 (s, 2H), 7.38 (d, $J = 2.1$ Hz, 1H), 7.30 (dd, $J = 8.4, 2.0$ Hz, 1H), 7.00 (d, $J = 8.4$ Hz, 1H), 3.90 (s, 6H), 3.84 (s, 3H), 3.76 (s, 3H). HR-MS (m/z) (ESI): calcd for $\text{C}_{19}\text{H}_{20}\text{O}_6$ [$\text{M}-\text{H}$] $^-$: 343.1182; found: 343.1064.

5.1.2. General procedure for preparing compounds **4** and **5**

Synthesis of compounds **4** and **5**. The compound **3** (10.0 mmol) was dissolved in anhydrous DMF (15 mL), and then anhydrous K_2CO_3 (20.0 mmol) and succinic anhydride (50.0 mmol) or glutaric anhydride (50.0 mmol) was added to the solution, respectively, and the mixture was stirred at 50 °C for 2 h and monitored by TLC. After confirming completion of the reaction, the solution was adjusted to pH = 2 ~ 3 with 4 N HCl. The resulting mixture was extracted with CH_2Cl_2 (3 \times 100 mL), and the organic phase was dried with anhydrous Na_2SO_4 . The resulting crude product was purified by silica gel column chromatography with $\text{CH}_3\text{OH}/\text{CH}_2\text{Cl}_2$ to obtain the final product **4** or **5**.

(*E*)-4-(2-methoxy-5-(3-oxo-3-(3,4,5-trimethoxyphenyl)prop-1-en-1-yl)phenoxy)-4-oxobutanoic acid (**4**). 2.8 g, 63.1% yield as a yellow solid. ^1H NMR (600 MHz, $\text{DMSO-}d_6$) δ 9.16 (s, 1H), 7.71 (d, $J = 15.4$ Hz, 1H), 7.63 (d, $J = 15.4$ Hz, 1H), 7.40 (s, 2H), 7.38 (d, $J = 2.1$ Hz, 1H), 7.31 – 7.29 (m, 1H), 7.00 (d, $J = 8.4$ Hz, 1H), 3.90 (s, 6H), 3.84 (s, 3H), 3.76 (s, 3H), 2.92 – 2.86 (m, 4H). HR-MS (m/z) (ESI): calcd for $\text{C}_{23}\text{H}_{24}\text{O}_9$ [$\text{M} + \text{Cl}$] $^-$

:479.1109; found: 479.0948.

(*E*)-5-(2-methoxy-5-(3-oxo-3-(3,4,5-trimethoxyphenyl)prop-1-en-1-yl)phenoxy)-5-oxopentanoic acid (**5**). 3.2 g, 69.9% yield as a yellow solid. ^1H NMR (400 MHz, $\text{DMSO-}d_6$) δ 12.18 (s, 1H), 7.86 – 7.81 (m, 2H), 7.74 – 7.69 (m, 2H), 7.42 (s, 2H), 7.19 (d, $J = 8.6$ Hz, 1H), 3.90 (s, 6H), 3.84 (s, 3H), 3.76 (s, 3H), 2.65 (t, $J = 7.3$ Hz, 2H), 2.39 (t, $J = 7.3$ Hz, 2H), 1.91 – 1.84 (m, 2H). HR-MS (m/z) (ESI): calcd for $\text{C}_{24}\text{H}_{26}\text{O}_9$ [$\text{M} + \text{Cl}$] $^-$: 493.1265; found: 493.1058.

5.1.3. General procedures for preparing complex **6** and **7**

To a solution of oxaliplatin (1.0 g 2.56 mmol) or DACHPt (1.0 g, 2.63 mmol) in water (30 mL) was dropwise added *N*-chlorosuccinimide (NCS) (534.1 mg, 4.0 mmol) in 10 mL water at room temperature. After that, the reaction solution was heated to 50 °C for 10 h. Process of the reaction was monitored with TLC and visualized with iodine in silica gel. Part of the solution was removed under reduced pressure, after completion of the reaction. The yellow crystal solid obtained was filtered, washed with water, cold ethanol and ether. Final target product was dried at dark in vacuum to give yellow solid.

Complex **6**. 974.8 mg. Yield 86.0%. Pale yellow solid. ^1H NMR (600 MHz, $\text{DMSO-}d_6$) δ 7.57–7.50 (m, 1H), 7.33–7.32 (m, 1H), 6.93 – 6.85 (m, 1H), 6.82–6.76 (m, 1H), 2.73–2.61 (m, 2H), 2.07– 2.02 (m, 2H), 1.50–1.47 (m, 4H), 1.39 (s, 1H), 1.05 – 0.96 (m, 2H).

Complex **7**. 1.04 g. Yield 90.0%. Pale yellow solid. ^1H NMR (600 MHz, $\text{DMSO-}d_6$) δ 7.94–7.93 (m, 1H), 7.72–7.71 (m, 1H), 7.21 – 7.12 (m, 1H), 7.05 – 6.98 (m, 1H), 2.97 (s, 1H), 2.56–2.50 (m, 2H), 2.03 (d, $J = 12.5$ Hz, 1H), 1.97 (d, $J = 12.1$ Hz, 1H), 1.55 – 1.40 (m, 4H), 1.11 – 1.03 (m, 2H).

5.1.4. General procedure for preparing compounds **8–11**

To a solution of **3** (0.35 mmol) or **4** (0.35 mmol) in anhydrous DMF (3 mL), and then TBTU (0.525 mmol), Et_3N (0.525 mmol) and complex **6** or **7** (0.35 mmol) was added in reaction, respectively and the resulting reaction was stirred at 30 °C for overnight. After confirming completion of the reaction, added to CH_2Cl_2 (150 mL) in solution, and then extracted twice with water (150 mL), and the organic phase was dried over anhydrous Na_2SO_4 . The residue was purified on silica gel column eluted $\text{CH}_3\text{OH}/\text{CH}_2\text{Cl}_2$ to obtain the desired products **8–11**.

(*OC*-6-33)-trichlorido(cyclohexane-1*R*,2*R*-diamine)(*E*)-4-(2-methoxy-5-(3-oxo-3-(3,4,5-trimethoxyphenyl)prop-1-en-1-yl)phenoxy)-4-oxobutanoate)-platinum(IV)(**8**). 167 mg, 58.9% yield as a yellow solid. ^1H NMR (600 MHz, $\text{DMSO-}d_6$) δ 9.49 – 9.46 (m, 1H), 8.10 – 7.98 (m, 1H), 7.82 (d, $J = 15.4$ Hz, 2H), 7.76 (d, $J = 7.8$ Hz, 2H), 7.69 (d, $J = 15.4$ Hz, 1H), 7.42 – 7.34 (m, 3H), 7.20 (d, $J = 8.3$ Hz, 1H), 2.86 – 2.78 (m, 2H), 2.66 – 2.56 (m, 3H), 2.14 (d, $J = 10.0$ Hz, 1H), 1.97 (d, $J = 10.2$ Hz, 1H), 1.49 – 1.17 (m, 5H), 1.01 – 0.77 (m, 2H). ^{13}C NMR (150 MHz, $\text{DMSO-}d_6$) δ 188.13, 181.60, 171.16, 153.39, 143.58, 142.41, 140.05, 133.54, 129.74, 128.13, 123.02, 120.69, 113.33, 106.62, 63.46, 62.54, 60.67, 56.80, 56.63, 32.30, 31.28, 31.24, 29.95, 24.00, 23.67. HR-MS (m/z) (ESI): calcd for $\text{C}_{29}\text{H}_{37}\text{Cl}_3\text{N}_2\text{O}_9\text{Pt}$ [$\text{M} + \text{H}$] $^+$: 859.1269; found: 859.0989. Elemental analysis calcd (%) for $\text{C}_{29}\text{H}_{37}\text{Cl}_3\text{N}_2\text{O}_9\text{Pt}$: C, 40.55; H, 4.34; N, 3.26; found: C, 40.78; H, 4.49; N, 3.01.

(*OC*-6-34)-chlorido(dicarboxylate)(cyclohexane-1*R*,2*R*-diamine)(*E*)-4-(2-methoxy-5-(3-oxo-3-(3,4,5-trimethoxyphenyl)prop-1-en-1-yl)phenoxy)-4-oxobutanoate)-platinum(IV)(**9**). 182 mg, 59.5% yield as a yellow solid. ^1H NMR (600 MHz, $\text{DMSO-}d_6$) δ 8.40 – 8.23 (m, 3H), 7.93 (d, $J = 32.4$ Hz, 1H), 7.79 – 7.66 (m, 4H), 7.44 (s, 2H), 7.19 (d, $J = 6.7$ Hz, 1H), 3.88 (s, 6H), 3.82 (s, 3H), 3.76 (s, 3H), 2.81 (d, $J = 18.9$ Hz, 2H), 2.68 – 2.55 (m, 3H), 2.08 (d, $J = 6.4$ Hz, 1H), 1.97 (d, $J = 8.8$ Hz, 1H), 1.50 – 1.23 (m, 5H), 1.09 – 0.92 (m, 2H). ^{13}C NMR (150 MHz, $\text{DMSO-}d_6$) δ 188.15, 179.56, 171.11, 163.84, 163.76, 153.38, 153.31, 143.65, 142.38, 140.09, 133.58, 130.21, 128.24, 122.67, 120.77, 113.19, 106.60, 61.86, 61.66, 60.66, 56.78, 56.60, 31.69, 31.32, 31.00, 29.81, 23.96, 23.79. HR-MS (m/z) (ESI): calcd for $\text{C}_{31}\text{H}_{37}\text{ClN}_2\text{O}_{13}\text{Pt}$ [$\text{M} + \text{Na}$] $^+$: 899.1524; found: 899.1266. Elemental analysis calcd (%) $\text{C}_{31}\text{H}_{37}\text{ClN}_2\text{O}_{13}\text{Pt}$ for: C, 41.41; H, 4.15; N, 3.12; found: C, 41.68; H,

4.36; N, 2.91.

(*OC-6-33*)-trichlorido(cyclohexane-1*R*,2*R*-diamine)((*E*)-5-(2-methoxy-5-(3-oxo-3-(3,4,5-trimethoxyphenyl)prop-1-en-1-yl)phenoxy)-5-oxopentanoate)-platinum(IV)(**10**). 175 mg, 57.6% yield as a yellow solid. ¹H NMR (400 MHz, DMSO-*d*₆) δ 9.60–9.51 (m, 1H), 8.23–8.07 (m, 1H), 7.86–7.81 (m, 3H), 7.75–7.69 (t, *J* = 12.4 Hz, 2H), 7.56–7.47 (m, 1H), 7.42 (s, 2H), 7.20 (d, *J* = 8.4 Hz, 1H), 3.90 (s, 6H), 3.84 (s, 3H), 3.76 (s, 3H), 2.76–2.65 (m, 3H), 2.47–2.37 (m, 2H), 2.19 (d, *J* = 10.0 Hz, 1H), 2.06 (d, *J* = 10.7 Hz, 1H), 1.90–1.86 (m, 2H), 1.56–1.40 (m, 3H), 1.31–1.02 (m, 4H). ¹³C NMR (100 MHz, DMSO-*d*₆) δ 188.14, 182.94, 171.42, 153.38, 143.58, 142.40, 140.15, 133.58, 129.90, 128.21, 122.74, 120.74, 113.30, 106.65, 63.90, 62.72, 60.67, 56.76, 56.65, 36.66, 32.88, 31.41, 31.33, 24.08, 24.03, 21.46. HR-MS (*m/z*) (ESI): calcd for C₃₀H₃₉Cl₃N₂O₉Pt [M+Na]⁺: 895.1245; found: 895.0971. Elemental analysis calcd (%) for C₃₀H₃₉Cl₃N₂O₉Pt: C, 40.21; H, 4.39; N, 3.13; found: C, 40.47; H, 4.62; N, 2.73.

(*OC-6-34*)-chlorido(dicarboxylate)(cyclohexane-1*R*,2*R*-diamine)((*E*)-5-(2-methoxy-5-(3-oxo-3-(3,4,5-trimethoxyphenyl)prop-1-en-1-yl)phenoxy)-5-oxopentanoate)-platinum(IV)(**11**). 183 mg, 58.8% yield as a yellow solid. ¹H NMR (400 MHz, DMSO-*d*₆) δ 8.44–8.28 (m, 3H), 7.88–7.83 (m, 2H), 7.73–7.69 (m, 3H), 7.42 (s, 2H), 7.20 (d, *J* = 8.6 Hz, 1H), 3.89 (s, 6H), 3.82 (s, 3H), 3.76 (s, 3H), 2.63–2.59 (m, 3H), 2.44 (t, *J* = 7.1 Hz, 2H), 2.11 (d, *J* = 10.8 Hz, 1H), 2.03 (d, *J* = 11.4 Hz, 1H), 1.88–1.82 (m, 2H), 1.57–1.33 (m, 4H), 1.25–1.06 (m, 3H). ¹³C NMR (100 MHz, DMSO-*d*₆) δ 188.11, 180.56, 171.27, 163.75, 153.38, 153.33, 143.60, 142.38, 140.11, 133.57, 130.06, 128.22, 122.65, 120.69, 113.25, 106.60, 62.00, 61.88, 60.66, 56.75, 56.57, 35.78, 32.78, 31.38, 31.05, 24.00, 24.91, 21.23. HR-MS (*m/z*) (ESI): calcd for C₃₂H₃₉ClN₂O₁₃Pt [M+Na]⁺: 913.1681; found: 913.1420. Elemental analysis calcd (%) for C₃₂H₃₉ClN₂O₁₃Pt: C, 42.09; H, 4.30; N, 3.07; found: C, 42.39; H, 4.51; N, 2.75.

5.2. In vitro cytotoxicity

The cytotoxicities of platinum(IV) complexes **8–11** against SK-OV-3, HCT-116, HepG-2, MCF-7, A549, SGC-7901, A549/CDDP and SGC-7901/CDDP were investigated by means of MTT assay, and the platinum(II) complexes and compound **3** were served as positive control. Culture medium Roswell Park Memorial Institute (RPMI-1640), phosphate buffered saline (PBS, pH = 7.2), fetal bovine serum (FBS), and Antibiotic-Antimycotic came from KeyGen Biotech Company (China). All cancer cell lines were cultivate in the supplemented with 10% FBS, and human normal liver cells LO2 were cultivate in the supplemented with 20% FBS, 100 units/ml of penicillin and 100 g/ml of streptomycin in a humidified atmosphere of 5% CO₂ at 37 °C. After that, the tested title compounds dissolved in DMF (Sigma), and diluted with a medium to five different concentrations. As for the negative control, 0.4% DMF was added. The cells were incubated in a humidified atmosphere of 5% CO₂ at 37 °C for 72 h. After that, added to 10 μM of MTT (5 mg/mL) in the cell culture fluid and the cells were incubated for another 4 h. After 4 h incubation, the medium was thrown away and replaced by 100 μL of DMSO (Sigma), and the O.D. value was read with a 570/630 nm enzyme-labeling instrument. The IC₅₀ values were calculated by SPSS software after three parallel experiments. Similarly, we also detected the cytotoxic effects of complex **11** (24 h and 48 h) against A549 and A549/CDDP cells via the same method mentioned above.

5.3. The stability of complex **11** in various conditions and intracellular analysis

For the sake to investigate the stability of compound **11** in various conditions. Solutions of **11** (50 μM) in PBS (150 mM) and acetonitrile (10 mL, 9.5:0.5, V/V), ascorbic acid (500 μM) in PBS (pH = 7.4, 150 mM), oxaliplatin (50 μM) and compound **5** (50 μM) were prepared. The experiments were carried out in dark at 37 °C and monitored via RP-HPLC (waters, e2695 system; 2489 UV/Vis detector). Upon mixing

with ascorbic acid (10 equiv.) the time-independent release with recorded every 1 h. Besides, a solution of complex **11** (50 μM) in DMF (containing 50% PBS, pH = 7.4), DMEM and DMEM + FBS were prepared and monitored at different time points of 0 h, 6 h, 24 h, 48 h and 72 h. All solutions were stored in dark at 37 °C. As for intracellular analysis, A549 cells were incubated with complex **11** (10 μM) for 24 h. After that, the cells were harvested, lysed and lysate was pre-filtered with microporous filter membrane (0.22 μm) for HPLC analysis. HPLC conditions: flow rate, 1.0 mL/min; detection wavelength, 254 nm; ODS column (250 × 4.6 mm, 5 μm), volume of sample injection, 10.0 μL; column incubator, 35 °C.

5.4. Cell uptake

A549 cells were seeded into 6-well plates at a density of 1 × 10⁶ cells/mL and allowed to adhere overnight until 80% confluence. After 24 h incubation, the cells were treated with oxaliplatin (10 μM) and **11** (5.0 and 10 μM) for another 12 h in the absence or presence of sodium azide (10 mM). After that, the cells were collected, and washed twice with ice PBS, and centrifuged at 1000 g, and resuspended in PBS (2 mL). So, the cell numbers were counted by using 200 μL suspension, and then the rest cells were digested with 65% HNO₃ at 65 °C for another 12 h. After that, the Pt level in A549 cells were analyzed by ICP-MS and the results were shown as one of three independent experiments.

5.5. Immunocytochemistry assay

A549 cells were seeded on glass coverslips at a density of 1 × 10⁶ cells/mL, allowed to adhere overnight and grew with **3** (10 μM), and **11** (5 and 10 μM) for another 24 h, using DMF as controls. After that, the cells were washed twice with ice PBS, fixed with paraformaldehyde (4%) for 20 min at room temperature, permeabilized with Triton X-100 (0.5% in PBS) and finally blocked with FBS for 1 h at room temperature. Then, the cells were labeled with antibody (α-tubulin) for 2 h, followed with IgG FITC conjugated antibody for 1 h. In order to track the cells, the cell nucleus stained with DAPI staining solution. The effects on microtubules polymerization of various compounds were recorded and analyzed with confocal laser microscope, and the results were shown as one of three independent experiments.

5.6. Cell apoptosis analysis

A549 cells were seeded into 6-well plates at a density of 1 × 10⁶ cells/mL and allowed to adhere overnight until 80% confluence. After 24 h incubation, the cells were treated with **3** (2.5 μM), oxaliplatin (10 μM), combined group (**3**, 2.5 μM, oxaliplatin, 10 μM), and **11** (2.5 and 5 μM) for another 24 h, using DMF as controls. After that, the cells were trypsinized, washed with ice PBS, suspended into 1 × binding buffer and doubled stained with annexin V-FITC and PI according to manufacture's protocol. Apoptosis results were recorded and analyzed with flow cytometry.

5.7. Cell cycle analysis

A549 cells were seeded into 6-well plates at a density of 1 × 10⁶ cells/mL and allowed to adhere overnight until 80% confluence. After 24 h incubation, the cells were treated with DMF, **3** (5 μM), oxaliplatin (10 μM), combined group (**3**, 5 μM, oxaliplatin, 10 μM), and **11** (2.5 and 5 μM) for another 24 h. After that, the cells were collected, washed with ice PBS and fixed with ice-cold ethanol at –20 °C overnight. Thereafter, the cells were washed with ice PBS, pre-incubated with RNase A (100 μg/mL) at 20 °C and collected to stain with propidium iodide (1 mg/mL) in dark at 4 °C for 30 min following with the illustrations of kits. The results of cell cycle assays were recorded and analyzed with flow cytometry.

5.8. Mitochondrial membrane potential (MMP) assay

A549 cells were seeded into 6-well plates at a density of 1×10^6 cells/mL and allowed to adhere overnight until 80% confluence. After 24 h incubation, the cells were treated with DMF, **3** (5 μ M), oxaliplatin (10 μ M), combined group (**3**, 5 μ M, oxaliplatin, 10 μ M), and **11** (2.5 and 5 μ M) for another 24 h. After that, the cells were trypsinized, washed with ice PBS and collected to stain with JC-1 fluorescent probe prepared previously according to the instructions of test kit. Thereafter, the cells were washed with ice PBS, collected at 2500 rpm and subjected to laser confocal microscope. The images of MMP changes were recorded and analyzed with laser confocal microscope with the 514, 585 and 529, 590 nm for excitation wavelength and emission wavelength, respectively, while the quantitative analysis was performed via flow cytometry.

5.9. Reactive oxygen species (ROS) assay

A549 cells were seeded into 6-well plates at a density of 1×10^6 cells/mL and allowed to adhere overnight until 80% confluence. Thereafter, the cells were incubated in triplicate with various compounds of vehicle (DMF), **3** (5 μ M), oxaliplatin (10 μ M), combined group (**3**, 5 μ M, oxaliplatin, 10 μ M), and **11** (2.5 and 5 μ M). After 24 h co-incubation, the cells were washed with cold PBS, collected and stained with Reactive Oxygen Species Assay Kit (DCFH-DA, Beyotime) at 25 °C in dark. The images of different groups were recorded and obtained with laser confocal microscope with excitation and emission wavelength of 505 nm and 535 nm, while the quantitative analysis was performed via flow cytometry.

5.10. Western blot assay

Western blot analysis was performed as described previously [39,42]. A549 cells were grown in a six-well plates at the density of 1×10^5 cells/mL of the RPMI-1640 medium with 10% FBS, and cultured until the cell density reached 80%. The tested compounds, including compound **3** (5 μ M), oxaliplatin (10 μ M), combined group (**3** + oxaliplatin, 5 + 10 μ M) and complex **11** (5 μ M) were dissolved by DMF (10 mM), and diluted in media to give the required concentrations (the final concentration of DMF was 0.2%) for the addition to the cells, and then the cells were cultured for another 24 h at 37 °C. So, the cells were treated with 0.2% DMF as for the negative control. After that, cells were washed ice-cold PBS, collected and centrifuged by 20000g at 4 °C for 10 min. The protein concentration in the supernatant was analyzed by the BCA protein assay reagents. Equal amounts of protein per line were separated by 8 ~ 12% sodium dodecyl sulfate–polyacrylamide gel electrophoresis (SDS-PAGE), and transferred to PVDF Hybond-P membrane (GE Healthcare). The membranes were incubated with 5% skim milk in Tris-buffered saline with Tween 20 (TBST) buffer for 1 h and then the membranes being gently rotated overnight at 4 °C. After that, the membranes were then incubated with primary antibodies against p53, Bcl-2, Bax, cleaved-Caspase-3, CHOP, p-eIF2 α and p-PERK or GAPDH at 4 °C for overnight. After that, the membranes washed with three times in TBST, and then the membranes were further incubated with peroxidase labeled secondary antibodies for another 2 h. After incubation, the washed with three times in TBST, and then the protein blots were detected by chemiluminescence reagent (Thermo Fischer Scientifics Ltd.), and the GAPDH was served as the loading control.

Declaration of Competing Interest

The authors declare that they have no known competing financial interests or personal relationships that could have appeared to influence the work reported in this paper.

Acknowledgements

We are grateful to the National Natural Science Foundation of China (Grant Nos. 21977021, 81760626 and 22007036), and the China Post-doctoral Science Foundation (2020M673553XB). In addition, we would like to thank the Natural Science Foundation of Guangxi Province (AB17292075) and Guangxi Funds for Distinguished Experts. Moreover, we are also very grateful to the Natural Science Foundation of Jiangsu Province (BK20191046) and the Open Project Program of the National & Local Joint Engineering Research Center for Mineral Salt Deep Utilization (SF201904) and the Open Project Program of the Jiangsu Key Laboratory of Regional Resource Exploitation and Medicinal Research (LPRK201902 and LPRK201904). Finally, we are also grateful to the Guangxi Natural Science Foundation of China (2019GXNSFBA245094) and the Youth Promotion Found of Guangxi (2019KY0386) and the Guangxi Science and Technology Base and Talents Program (AD19110109).

Appendix A. Supplementary material

Supplementary data to this article can be found online at <https://doi.org/10.1016/j.bioorg.2021.104741>.

References

- [1] N.J. Wheate, S. Walker, G.E. Craig, R. Oun, The status of platinum anticancer drugs in the clinic and in clinical trials, *Dalton Trans.* 39 (2010) 8113–8127.
- [2] L. Kelland, The resurgence of platinum-based cancer chemotherapy, *Nat. Rev. Cancer.* 7 (2007) 573–584.
- [3] K.B. Huang, F.Y. Wang, X.M. Tang, H.W. Feng, Z.F. Chen, Y.C. Liu, Y.N. Liu, H. Liang, Organometallic gold(III) complexes similar to tetrahydroisoquinoline induce ER-stress-mediated apoptosis and pro-death autophagy in A549 cancer cells, *J. Med. Chem.* 61 (2018) 3478–3490.
- [4] W. Liu, R. Gust, Metal N-heterocyclic carbene complexes as potential antitumor metalodrugs, *Chem. Soc. Rev.* 42 (2013) 755–773.
- [5] X. Qin, L. Fang, F. Chen, S. Gou, Conjugation of platinum(IV) complexes with chlorambucil to overcome cisplatin resistance via a “joint action” mode toward DNA, *Eur. J. Med. Chem.* 137 (2017) 167–175.
- [6] X.P. Han, S. Jin, Y.J. Wang, Z.G. He, Recent advances in platinum(IV) complex based delivery systems to improve platinum(II) anticancer therapy, *Med. Res. Rev.* 35 (2015) 1268–1299.
- [7] T.C. Johnstone, K. Suntharalingam, S.J. Lippard, The next generation of platinum drugs: targeted Pt(II) agents, nanoparticle delivery, and Pt(IV) prodrugs, *Chem. Rev.* 116 (2016) 3436–3486.
- [8] L. Fang, X. Qin, J. Zhao, S. Gou, Construction of dual stimuli-responsive platinum (IV) hybrids with NQO1 targeting ability and overcoming cisplatin resistance, *Inorg. Chem.* 58 (2019) 2191–2200.
- [9] V. Lira-Peurto, A. Silva, M. Morris, et al., Phase II trial of carboplatin or iproplatin in cervical cancer, *Canc. Chemoth. Pharm.* 28 (1991) 391–396.
- [10] U. Basu, B. Banik, R. Wen, R.K. Pathak, S. Dhar, The Platin-X series: activation, targeting, and delivery, *Dalton Trans.* 45 (2016) 12992–13004.
- [11] J. O'Rourke, R. Weiss, P. New, et al., Phase I clinical trial of ormaplatin (tetraplatin, NSC 363812), *Anticancer Drugs* 5 (1994) 520–526.
- [12] E. Wexselblatt, D. Gibson, What do we know about the reduction of Pt(IV) prodrugs? *J. Inorg. Biochem.* 117 (2012) 220–229.
- [13] R.J. Boohaker, M.W. Lee, P. Vishnubhotla, J.M. Perez, A.R. Khaled, The use of therapeutic peptides to target and to kill cancer cells, *Curr. Med. Chem.* 19 (2012) 3794–3804.
- [14] N. Graf, T.E. Mokhtari, I.A. Papayannopoulos, S.J. Lippard, Platinum(IV)-chlorotoxin (CTX) conjugates for targeting cancer cells, *J. Inorg. Biochem.* 110 (2012) 58–63.
- [15] (a) Y. Kido, A.R. Khokhar, Z.H. Siddik, Glutathione-mediated modulation of tetraplatin activity against sensitive and resistant tumor cells, *Biochem. Pharmacol.* 47 (1994) 1635–1642; (b) M.D. Hall, T.W. Hambley, Platinum(IV) antitumor compounds: their bioinorganic chemistry, *Coord. Chem. Rev.* 232 (2002) 49–67.
- [16] (a) G.R. Gibbons, S. Wyrick, S.G. Chaney, Rapid reduction of tetrachloro(D, L-trans) 1,2-diaminocyclohexaneplatinum(IV) (tetraplatin) in RPMI 1640 tissue culture medium, *Cancer Res.* 49 (1989) 1402–1407; (b) W. Zhong, Q. Zhang, Y. Yan, S. Yue, B. Zhang, W. Tang, Reaction of a platinum (IV) complex with native Cd, Zn-metallothionein in vitro, *J. Inorg. Biochem.* 66 (1997) 179–185.
- [17] R. Romagnoli, P.G. Baraldi, M.D. Carrion, O. Cruz-Lopez, C.L. Cara, J. Balzarini, E. Hamel, A. Canella, E. Fabbri, R. Gambari, G. Basso, Hybrid a-bromoacryloylamido chalcones. Design, synthesis and biological evaluation, *Bioorg. Med. Chem. Lett.* 19 (2009) 2022–2028.
- [18] R. Pingaew, A. Saekee, P. Mandi, C. Nantasenamat, S. Prachayasittikul, S. Ruchirawat, V. Prachayasittikul, Synthesis, biological evaluation and molecular

- docking of novel chalconecoumarin hybrids as anticancer and antimalarial agents, *Eur. J. Med. Chem.* 85 (2014) 65–76.
- [19] Y. Kong, K. Wang, M.C. Edler, E. Hamel, S.L. Mooberry, M.A. Paige, M.L. Brown, A boronic acid chalcone analog of combretastatin A-4 as a potent antiproliferation agent, *Bioorg. Med. Chem.* 18 (2010) 971–977.
- [20] C. Zhu, Y. Zuo, R. Wang, B. Liang, X. Yue, G. Wen, N. Shang, L. Huang, Y. Chen, J. Du, X. Bu, Discovery of potent cytotoxic orthoaryl chalcones as new scaffold targeting tubulin and mitosis with affinitybased fluorescence, *J. Med. Chem.* 57 (2014) 6364–6382.
- [21] H. Mirzaei, S. Emami, Recent advances of cytotoxic chalconoids targeting tubulin polymerization: Synthesis and biological activity, *Eur. J. Med. Chem.* 121 (2016) 610–639.
- [22] P. Singh, A. Anand, V. Kumar, Recent developments in biological activities of chalcones: A mini review, *Eur. J. Med. Chem.* 85 (2014) 758–777.
- [23] W. Wu, H. Ye, L. Wan, X. Han, G. Wang, J. Hu, M. Tang, X. Duan, Y. Fan, et al., Millepachine, a novel chalcone, induces G2/M arrest by inhibiting CDK1 activity and causing apoptosis via ROS-mitochondrial apoptotic pathway in human hepatocarcinoma cells in vitro and in vivo, *Carcinogenesis* 34 (2013) 1636–1643.
- [24] G.C. Wang, F. Peng, D. Cao, Z. Yang, X.L. Han, J. Liu, W.S. Wu, L. He, L. Ma, J. Y. Chen, Y. Sang, M.L. Xiang, A.H. Peng, Y.Q. Wei, L.J. Chen, Design, synthesis and biological evaluation of millepachine derivatives as a new class of tubulin polymerization inhibitors, *Bioorg. Med. Chem.* 21 (2013) 6844–6854.
- [25] R. Schobert, B. Biersack, A. Dietrich, S. Knauer, M. Zoldakova, A. Fruehauf, T. Mueller, Pt(II) complexes of a combretastatin A-4 analogous chalcone: effects of conjugation on cytotoxicity, tumor specificity, and long-term tumor growth suppression, *J. Med. Chem.* 52 (2009) 241–246.
- [26] S. Ducki, R. Forrest, J.A. Hadfield, A. Kendall, N.J. Lawrence, A.T. McGown, D. Rennison, potent antimitotic and cell growth inhibitory properties of substituted chalcones, *Bioorg. Med. Chem. Lett.* 8 (1998) 1051–1056.
- [27] M. Ravera, E. Gabano, G. Pelosi, F. Fregonese, S. Tinello, D. Osella, A new entry to asymmetric platinum(IV) complexes via oxidative chlorination, *Inorg. Chem.* 53 (2014) 9326–9335.
- [28] X.Q. Song, Z.Y. Ma, Y.G. Wu, M.L. Dai, D.B. Wang, J.Y. Xu, Y. Liu, New NSAID-Pt(IV) prodrugs to suppress metastasis and invasion of tumor cells and enhance anti-tumor effect in vitro and in vivo, *Eur. J. Med. Chem.* 167 (2019) 377–387.
- [29] (a) C. Qian, J.Q. Wang, C.L. Song, L.L. Wang, L.N. Ji, H. Chao, The induction of mitochondria-mediated apoptosis in cancer cells by ruthenium(II) asymmetric complexes, *Metallomics.* 5 (2013) 844–854;
(b) S. Mayor, R.E. Pagano, Pathways of clathrin-independent endocytosis, *Nat. Rev. Mol. Cell Biol.* 8 (2007) 603–612;
(c) H.C. Lichstein, Studies of the effect of sodium azide on microbic growth and respiration, *J. Bacteriol.* 47 (1944) 239–251.
- [30] X.C. Huang, M. Wang, C.G. Wang, W.W. Hu, Q.H. You, T. Ma, Q. Jia, C.H. Yu, Z. X. Liao, H.S. Wang, Synthesis and biological evaluation of novel millepachine derivative containing aminophosphonate ester species as novel anti-tubulin agents, *Bioorg. Chem.* 94 (2020) 103486.
- [31] M. Tian, J. Li, S. Zhang, L. Guo, X. He, D. Kong, H. Zhang, Z. Liu, Half-sandwich ruthenium (ii) complexes containing N^Nchelated imino-pyridyl ligands that are selectively toxic to cancer cells, *Chem. Commun.* 53 (2017) 12810–12813.
- [32] J.S. Clerkin, R. Naughton, C. Quiney, T.G. Cotter, Mechanisms of ROS modulated cell survival during carcinogenesis, *Canc. Lett.* 266 (2008) 30–36.
- [33] H.M.A. Zeeshan, G.H. Lee, H.R. Kim, H.J. Chae, Endoplasmic reticulum stress and associated ROS, *Int. J. Mol. Sci.* 17 (2016) 327–346.
- [34] H.U. Simon, A. Haj-Yehia, F. Levi-Schaffer, Role of reactive oxygen species (ROS) in apoptosis induction, *Apoptosis* 5 (2000) 415–418.
- [35] Y. Gou, J. Wang, S.F. Chen, Z. Zhang, Y. Zhang, W. Zhang, F. Yang, a-Nheterocyclic thiosemicarbazone Fe(III) complex: Characterization of its antitumor activity and identification of anticancer mechanism, *Eur. J. Med. Chem.* 123 (2016) 354–364.
- [36] N.N. Danial, S.J. Korsmeyer, Cell death: critical control points, *Cell* 116 (2004) 205–219.
- [37] Y.L. Chu, C.T. Ho, J.G. Chung, R. Rajasekaran, L.Y. Sheen, Allicin induces p53-mediated autophagy in HepG2 human liver cancer cells, *J. Agric. Food Chem.* 60 (2012) 8363–8371.
- [38] P. Monian, X. Jiang, Clearing the final hurdles to mitochondrial apoptosis: regulation post cytochrome c release, *Exp. Oncol.* 34 (2012) 185–191.
- [39] Z. Liu, M. Wang, H. Wang, L. Fang, S. Gou, Targeting RAS-RAF pathway significantly improves antitumor activity of Rigosertib-derived platinum(IV) complexes and overcomes cisplatin resistance, *Eur. J. Med. Chem.* 194 (2020) 112269.
- [40] B. Englinger, C. Pirker, P. Heffeter, A. Terenzi, C.R. Kowol, B.K. Keppler, W. Berger, Metal drugs and the anticancer immune response, *Chem. Rev.* 119 (2019) 1519–1624.
- [41] B. Al-Lazikani, U. Banerji, P. Workman, Combinatorial drug therapy for cancer in the post-genomic era, *Nat. Biotechnol.* 30 (2012) 679–692.
- [42] S.H. Huang, L.W. Wu, A.C. Huang, C.C. Yu, J.C. Lien, Y.P. Huang, J.S. Yang, J. H. Yang, Y.P. Hsiao, W.G. Wood, C.S. Yu, J.G. Chung, Benzyl isothiocyanate (BITC) induces G2/M phase arrest and apoptosis in human melanoma A375.S2 cells through reactive oxygen species (ROS) and both mitochondria dependent and death receptor-mediated multiple signaling pathways, *J. Agric. Food Chem.* 60 (2012) 665–675.